25th ABCM International Congress of Mechanical Engineering
October 20-25, 2019, Uberlândia, MG, Brazil

COB-2019-2413
MECHANICAL, THERMAL AND FATIGUE PROPERTIES OF GLASS FIBER REINFORCED POLYAMIDE 6 COMPOSITE AS A SUBSTITUTION FOR STEEL FOR WEIGHT REDUCTION OF VEHICLES

Martin Ferreira Fernandes
Roberto Ferreira Motta Jr.
Mariana de Lima Cardoso
Maria Odila Hilário Cioffi
Herman Jacobus Cornelis Voorwald
Sao Paulo State University (Unesp), School of Engineering, Guaratingueta. 12516-410. Sao Paulo, Brazil
martin.fernandes@unesp.br, roberto.motta@unesp.br, mariana_lcardoso@hotmail.com, odila.cioffi@unesp.br, h.voorwald@unesp.br

Abstract. *The weight reduction of structural automotive components is important for the automotive industry considering the energy efficiency, fuel consumption and the further increasing rigorous environment restrictions concerning the CO_2 emission of vehicles. The employment of lightweight materials, such as polymer composites, is an effective way to reduce the weight of vehicles. The mechanical, fatigue and thermal properties of 60% glass fiber reinforced polyamide 6 (PA6/G60) were investigated and compared to LNE 500 steel properties. The feasibility of the substitution of LNE 500 steel for PA6/G60 in an automotive stringer structure was evaluated. Axial fatigue tests were performed for both materials at room temperature. Fracture surfaces were observed through scanning electron microscopy. Flexural tests at perpendicular and parallel directions to the fiber orientation, thermogravimetric analysis, and differential scanning calorimetry were carried out for the PA6/G60 composite. The finite element method was used to obtain the stress distribution in an automotive stringer with the substitution of part of the structure for the composite. The results showed that the PA6/G60 composite has lower mechanical, thermal and fatigue properties than LNE 500 steel. The substitution of steel for lightweight composite materials for automotive structural applications may lead to the necessity of new design concepts.*

Keywords: *polymer composites, glass fiber, fatigue, finite element method, polyamide 6*

1. INTRODUCTION

Lightweight manufacturing is fundamental for the automotive industry considering the strict and further increasing rigorous environment restrictions concerning the amount of harmful gases (Tisza and Czinege, 2018). Among the regulations to reduce CO_2 emission per km, the European Union adopted a regulation called EURO 6 from 2020 that will apply a high tax to vehicles exceeding 95 g/km of CO_2 emission, which only a few types of existing automobiles satisfy (Ishikawa et al., 2018). The weight reduction of structural automotive parts improve energy efficiency and reduces the CO_2 emission of vehicles. The weight reduction is also correlated to the amount of fuel that the vehicle consumes. The reduction of 4 kg in the mass of a midsized car saves up to 36 L of fuel and 75 kg of CO_2 emission during a vehicle's useful life (Teixeira et al., 2015). Even for electric cars, the application of lightweight materials is important since, when producers add heavier batteries to the vehicles, other components have to become lighter (O'Brien-Bernini, 2011).

The environmental regulations to produce more eco-friendly vehicles are related to a global trend of sustainability and energy efficiency. Considering this worldwide scenario, the concept of sustainability in the automotive industry is also relevant to the company's reputation and attractiveness on the sales market (Koplin et al., 2007). Sustainability is a concept that requires a balance of economic, human and environmental factors to meet our needs without compromising the resources for future generations (O'Brien-Bernini, 2011). Sustainability is a critical issue for the automotive industry considering the global growth of vehicles and fuel demand. For example, in the period from 1960 to 2002, the total vehicle ownership in the world has increased from 122 to 812 million (Mayyas et al., 2012).

Kampe (2001) developed a model to include energy consumption before and during service in the material selection. The method is based on the use of the classical Ashby mass-based material selection indices with modifications to include the energy consumption. The equation to compute the required mass for a set of conditions can be derived for different components. For example, Eq. (1) computes the mass of a beam to withstand the loading without overload

failure for a 2:1 cross-sectional aspect ratio, where L is the length, W is the uniformly-distributed load, ρ is the specific mass, and σ_f is the failure strength (Kampe, 2001). Note that ρ and σ_f are material properties, which allow the calculation of a mass index from those two variables for different materials.

$$m = \left(\frac{3}{4\sqrt{2}} \cdot W \cdot L^{7/2}\right)^{2/3} \cdot \left(\frac{\rho}{\sigma_f^{2/3}}\right) \quad (1)$$

The lifetime energy consumption (LEC) can be obtained through the summation of two components (i) the energy expenditure required to assure the beam availability for the design, by multiplying the derived mass by the energy content, q, and (ii) the energy consumed over lifetime of vehicle (Kampe, 2001). Equation (2) shows the LEC index (LEC′) that depends on the material properties.

$$LEC' = \frac{\rho \cdot q}{\sigma^{2/3}} + C_E \cdot \frac{\rho}{\sigma^{2/3}} \quad (2)$$

The alternatives to reduce the weight of vehicles include the employment of lighter materials, the increase of functionality of components and innovations in the car system design. The employment of lightweight materials is the most direct and effective way to reduce the weight of vehicles (Ishikawa et al., 2018). The metallic trending materials to produce lightweight automotive parts are high strength steels and high strength aluminum alloys (Tisza and Czinege, 2018). The substitution of steel or even aluminum parts for composites materials in automotive components can reduce even more the weight of vehicles. For example, the substitution of car chassis made of aluminum alloy for carbon fiber reinforced thermoplastic composites can achieve 10% weight reduction with the same rigidity (Ishikawa et al., 2018).

Thermoplastic composites combine ease of processing, good resistance to corrosion, low specific mass, and recyclability (Teixeira et al., 2015). Automotive parts are shifting from metals to composite materials made with thermoplastic matrix, such as glass fiber reinforced polyamide (Mouti et al., 2013). Among various types of polyamide commercially available, polyamide 6 (PA6) is one of the polyamide grades most used in the automotive industry (Gendre et al. 2015). Recently, some studies concerning mechanical properties of polyamide 6 composites were conducted. Güllü et al. showed that 15 and 30 wt% of glass fiber reinforcement increases the tensile strength value of PA6 in about 74 and 111%, respectively. Gendre et al. (2015) found out that the addition of nano-fillers deteriorated the tensile properties of polyamide 6 nanocomposites with 30% of short-fibers reinforcement.

The automotive industry concern of substitution of steel for lightweight materials has led to recent studies on this area. Güler et al. (2018) developed a lightweight design of an automobile hinge component using a glass fiber polyamide composite as a substitution for steel. Teixeira et al. (2015) determined the injection process parameters to maximize the flexural strength and surface quality of long glass fiber-reinforced polyamide 6.6 composites aiming automotive applications. The interest for discontinuous fiber-reinforced composites is justified considering the good productivity and suitability for complex geometry automotive components. The fiber-reinforced composite components are usually produced using injection molding techniques (Sasayama et al. 2013). Sasayama et al. (2013) showed that the fiber length and orientation distributions influence the failure properties of short glass fiber-reinforced polyamide 6.6.

Automotive components are subjected to vibratory loads, which may result in the fatigue process. Therefore, the fatigue strength is an important property to mechanical components in vehicles and it has to be evaluated to apply the material in a structural component and avoid the fatigue crack nucleation and propagation until the fracture of the component. Bernasconi et al. (2007) studied the effect of fiber orientation on the fatigue behavior of a short glass fiber reinforced polyamide 6, indicating decreasing values of ultimate tensile stress and fatigue strength for increasing values of the orientation angle of specimens.

This present study aims to investigate the feasibility of the substitution of LNE 500 steel for 60% glass fiber reinforced polyamide 6 (PA6/GF60) at automotive stringers. The mechanical, fatigue and thermal properties of PA6/GF60 composite were evaluated to enable the application of the material in automotive parts aiming for weight reduction of vehicles.

2. MATERIALS AND METHODS

2.1 Materials

The LNE 500 steel and the 60% glass fiber reinforced polyamide 6 (PA6/GF60) were received from Maxion Structural Components, Brazil. The steel specimens were machined from 4 mm thick plates. The chemical composition of LNE 500 steel used in this work is shown in Table 1. The composite 3 mm thick plates were processed by injection molding technique by Lanxess, Germany, and supplied to Maxion SC. The composite was composed of 40% of polyamide 6 matrix and 60% content by weight of short glass fiber reinforcement.

Table 1. Composition of LNE 500 steel.

C (%)	Mn (%)	Si (%)	P (%)	S (%)	Al (%)	Nb (%)	V (%)	Ti (%)
0.12	1.50	0.35	0.025	0.015	0.015	0.12	0.12	0.20

2.2 Methods

The methodology proposed in this work aims at investigating the feasibility of the substitution of LNE 500 steel for PA6/GF60 at automotive stringers and other vehicle components, considering the necessity of weight reduction of vehicles.

Optical microscopy was used to characterize the microstructure of LNE steel. After metallographic preparation, the chemical etching used was Nital 3%. Mechanical properties relevant to the application of LNE 500 steel were obtained. Tensile tests in LNE 500 steel followed ASTM E8 standard. Axial fatigue tests were carried out with a stress ratio R = 0.1 and frequency f = 20 Hz at room temperature in specimens according to ASTM E466 in an Instron 8801 until fracture or 10^6 cycles. A scanning electron microscope (SEM) LEO model 1450-VP was used to obtain the fracture surfaces.

The PA6/GF60 composite properties were evaluated through mechanical tests and thermal analysis. The tensile tests were carried out in the parallel direction to the orientation of fibers in specimens with dimensions of (64 x 7.5 x 3) mm. Axial fatigue tests were carried out with a stress ratio R = 0.1 and frequency f = 20 Hz at room temperature in specimens with dimensions of (64 x 7.5 x 3) mm in an Instron 8801 until fracture or 10^6 cycles. SEM was used to obtain the fracture surfaces. Three-point flexural tests were carried out, according to ASTM D790, using a Shimadzu AG-X test machine with the loading applied in the parallel and perpendicular directions to the short glass fibers orientation.

The thermogravimetric analysis (TGA) and derivative thermogravimetry (DTG) were performed using SII Nanotechnology INC model Exstar 6000 with a 10 °C/min heating rate between 25 °C and 800 °C, under nitrogen atmosphere. The differential scanning calorimetry (DSC) was performed using DSC Q20 TA Instruments with the following steps: (i) 10 °C/min heating rate between 0 °C and 300 °C, (ii) 10 °C/min cooling rate between 300 °C and 0 °C, and (iii) 10 °C/min heating rate between 0 °C and 300 °C.

The finite element method (FEM) was used to perform a structural analysis using the software *HyperWorks* to obtain the stress gradient in an automotive stringer with the substitution of LNE 500 steel for PA6/GF60 composite in part of the structure. The stringer model is shown in Fig. 1, where the brown structure is made of PA6/GF60 composite as a substitution for LNE 500 steel. The material substitution in the original project made only of LNE 500 steel would reduce the weight of the stringer from approximately 7.0 kg to 3.5 kg. Two conditions were tested in the FEA, a pair of 500 N and a pair of 1,000 N forces applied in opposite directions to the stringer to generate a torque.

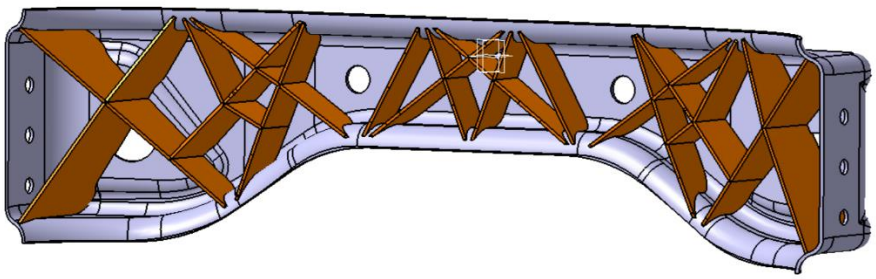

Figure 1. Automotive stringer model with the substitution of LNE 500 steel for PA6/GF60 composite (Maxion SC prototype).

3. RESULTS AND DISCUSSION

3.1 Microstructure characterization of LNE 500 steel

The microstructure of LNE 500 steel after Nital 3% etching is shown in Fig. 1. The larger grains are formed by ferrite, which can be identified by the light color, while the structure identified by the darker color is pearlite. The ferrite phase is responsible for the ductility of the material, while pearlite is responsible for the mechanical strength.

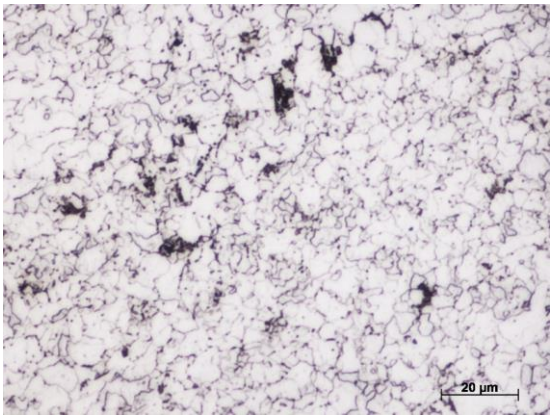

Figure 2. Microstructure of LNE 500 steel.

3.2 Tensile tests

The ultimate tensile strength of LNE 500 steel and PA6/G60 composite were (521.8 ± 8.7) MPa and (147.3 ± 3.8) MPa, respectively. As expected, the tensile properties of LNE 500 are superior to PA6/G60. However, the material selection for a component can be made considering other variables, such as the mass-based material selection indices calculated from Eq. (1). In order to compute the mass index, it was assumed that (i) the specific mass of LNE 500 steel and PA6/G60 are 7.8 g/cm^3 and 1.71 g/cm^3, respectively, and (ii) the failure strength is the ultimate tensile strength obtained in the tensile tests for both materials. Thus, the mass index $\rho/\sigma_f^{2/3}$ obtained were 280 (kg/m^3 MPa$^{2/3}$) for the LNE 500 steel and 26 (kg/m^3 MPa$^{2/3}$) for the PA6/G60 composite. These results indicate the weight reduction potential of applying PA6/G60 composite for automotive components as a substitution for original projects with steel. Besides, it also represents the potential for lifetime energy consumption reduction.

3.3 Flexural tests

The flexural tests results of PA6/GF60 composite are shown in Fig 3. The flexural strength for loadings applied in the parallel and perpendicular directions were (225.2 ± 5.2) MPa and (132.8 ± 14.7) MPa, respectively. It is possible to observe that the flexural test curves were more uniform for loadings applied in the parallel direction to the fiber orientation and that the standard deviation of the flexural strength was higher for the perpendicular direction. The tests showed that the composite has better flexural strength in the parallel direction (Fig. 3a) to the fiber orientation than perpendicular direction (Fig. 3b). The difference in the behavior is explained because the fibers subjected to tensile loadings are responsible for the strength of composites.

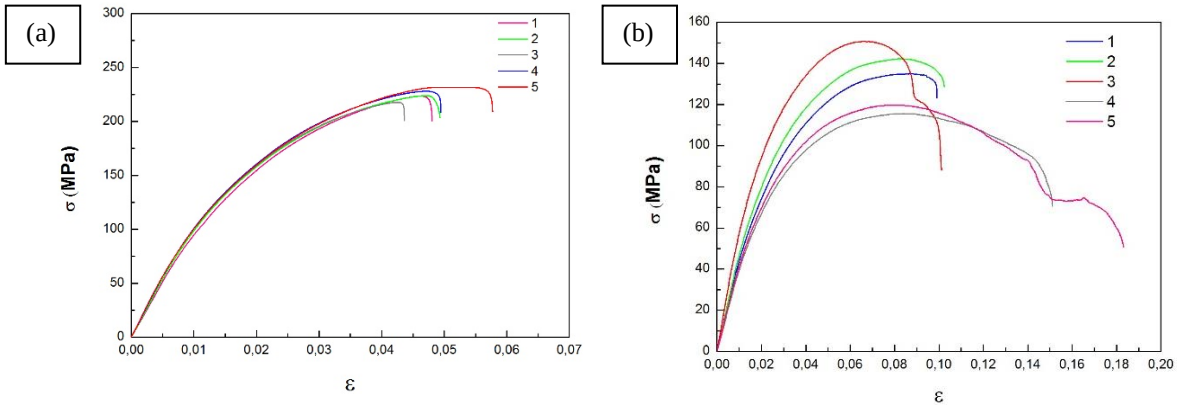

Figure 3. Flexural test curves of PA6/GF60 composite for (a) loading applied in the parallel direction to the fiber orientation (b) loading applied in the perpendicular direction to the fiber orientation.

3.4 Thermogravimetric analysis (TGA)

The TGA is a technique in which the mass change of the composite was measured as a function of the temperature. Figure 4 shows the thermogravimetric curve obtained for PA6/GF60 composite and the DTG curve, which is the first

derivative of the TGA curve. The PA6/GF60 composite showed thermal stability up to about 350 °C since the mass loss was negligible below this temperature. Beyond this temperature, the material began to degrade. The mass loss comes from the release of water and organic volatiles as the temperature increases. As observed in the DTG curve, degradation occurs more intensely at 450 °C. For temperatures above 480 °C, about 40% of the material is degraded, which corresponds to the polyamide 6 portion of the composite. Considering only the thermal stability of the material obtained in TGA, the maximum temperature that the material could be applied would be 350 °C. However, the DSC thermal analysis will be presented in the following section to obtain more properties.

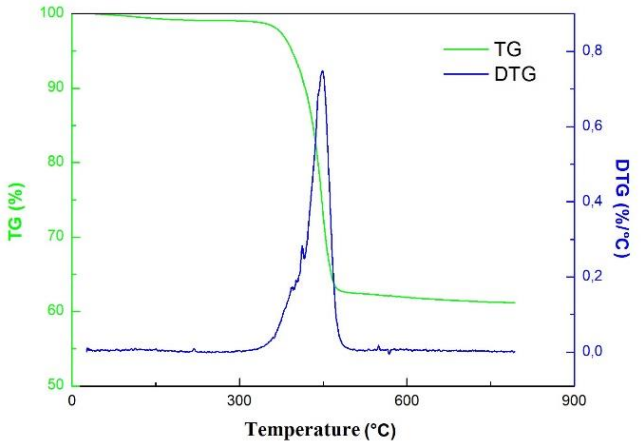

Figure 4. Thermogravimetric curves (TGA and DTG) for PA6/GF60 composite.

3.5 Differential Scanning Calorimetry (DSC)

The DSC curves present the heat flow changes as a function of temperature. Figure 5a shows the DSC curves for the first heating between 0 °C and 300 °C and the cooling between 300 °C and 0 °C. Figure 5b shows the DSC curve for the second heating between 0 °C and 300 °C. From the first heating curve (Fig. 5a), the fusion starts at 205 °C and ends at 230 °C. The endothermic peak was identified at 224.8 °C, which is the melting point (T_m). The existence of the T_m is justified since the polyamide 6 matrix is a semi-crystalline polymer. From the cooling curve (Fig. 5a), an exothermic peak occurs at a different temperature from T_m. This is the crystallization temperature (T_c), which was identified at 180.8 °C. T_c is a transition from amorphous solid to crystalline solid. From the second heating curve (Fig. 5b), the T_m occurred at 223 °C, which is almost similar to the result obtained in the first heating curve. The enthalpy of transition (ΔH) for fusion and crystallization was obtained integrating the peak corresponding to each transition.

The glass transition temperature (T_g) is the reversible transition in the polyamide 6 matrix from a hard "glassy" state into a viscous state as the temperature increases. The T_g was obtained through DSC signal as the temperature at which the baseline changes during the first heating, which is approximately 63 °C. The T_g temperature of the material is relatively low and it may be a critical factor considering that the automotive stringer may reach higher temperatures. Finally, Table 2 presents a summary of the thermal properties obtained in DSC.

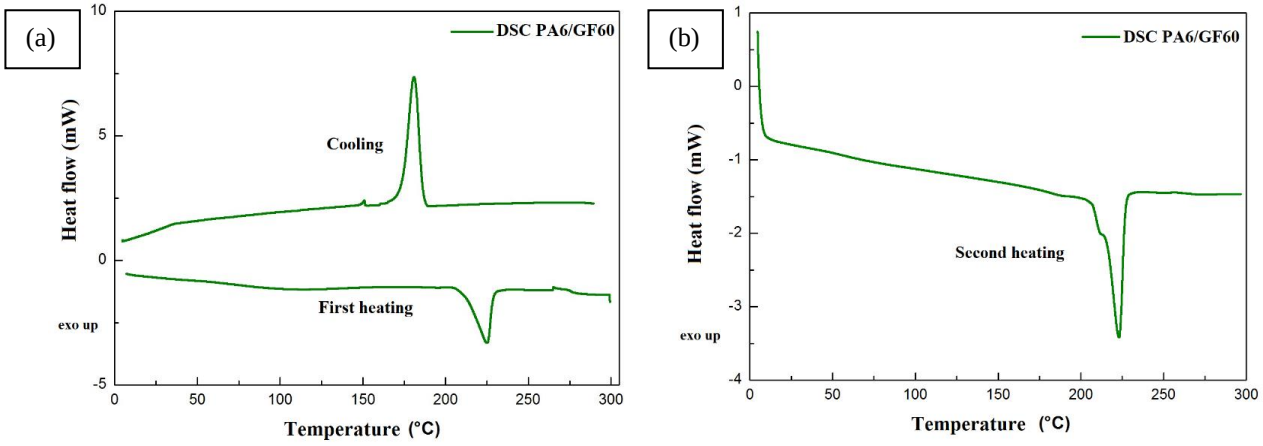

Figure 5. DSC curves for PA6/GF60 composite (a) first heating between 0 °C and 300 °C and cooling between 300 °C and 0 °C, and (b) second heating between 0 °C and 300 °C.

Table 2. Properties obtained in DSC of PA6/GF60 composite.

Material	T_f (1º)	T_f (2º)	T_c	ΔH_f (1º)	ΔH_f (2º)	ΔH_c	T_g
PA6/GF60	224.8 °C	223 °C	180.8 °C	25.2 J/g	19.7 J/g	23.3 J/g	63 °C

3.6 Fatigue tests

The stress-life curve (S-N curve) of the LNE 500 steel is shown in Fig. 6. The maximum stress level tested varied from 95% to 75% of the ultimate tensile strength. Equation (3) was obtained to predict the fatigue life (N) of the LNE 500 steel from a maximum fatigue stress level given in MPa (σ).

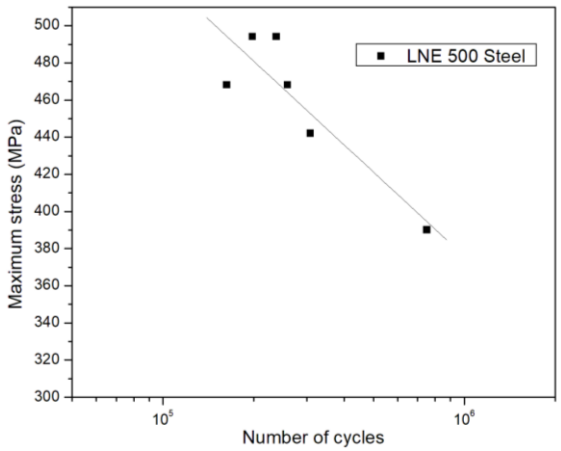

Figure 6. S-N curve of the LNE 500 steel.

$$\sigma = 1276.78 - 150.14 \log N \quad (3)$$

The S-N curve of the PA6/GF60 composite is shown in Fig. 6. The maximum stress level tested varied from 95% to 75% of the ultimate tensile strength. Similarly to Eq. (3), Eq. (4) can estimate the fatigue life (N) of the PA6/GF60 composite. It can be observed that the substitution of LNE steel for PA6/GF60 composite would result in a significant reduction of the fatigue strength of the component.

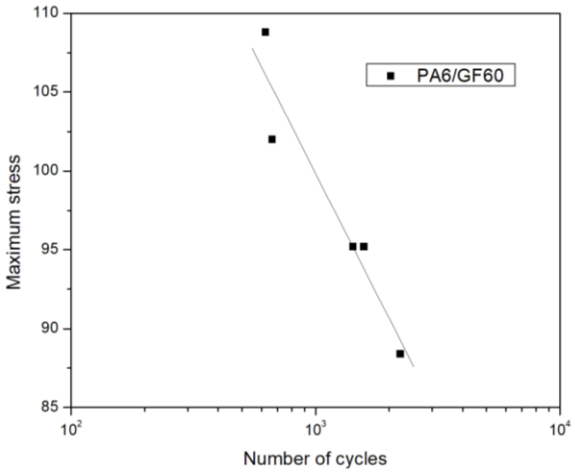

Figure 7. S-N curve of the PA6/GF60 composite.

$$\sigma = 191.34 - 30.49 \log N \quad (4)$$

3.7 Fracture surfaces

The typical fatigue fracture surface of LNE 500 steel specimens is presented in Fig. 8. Figure 8a shows the crack nucleation source at the surface. The nucleation occurs at the surface due to higher local cyclic plastic strain as a consequence of the stress concentration effect and the reduced constraint of the free surface. Figure 8b shows the dimples in the final fracture region, which is related to the ductility of the material.

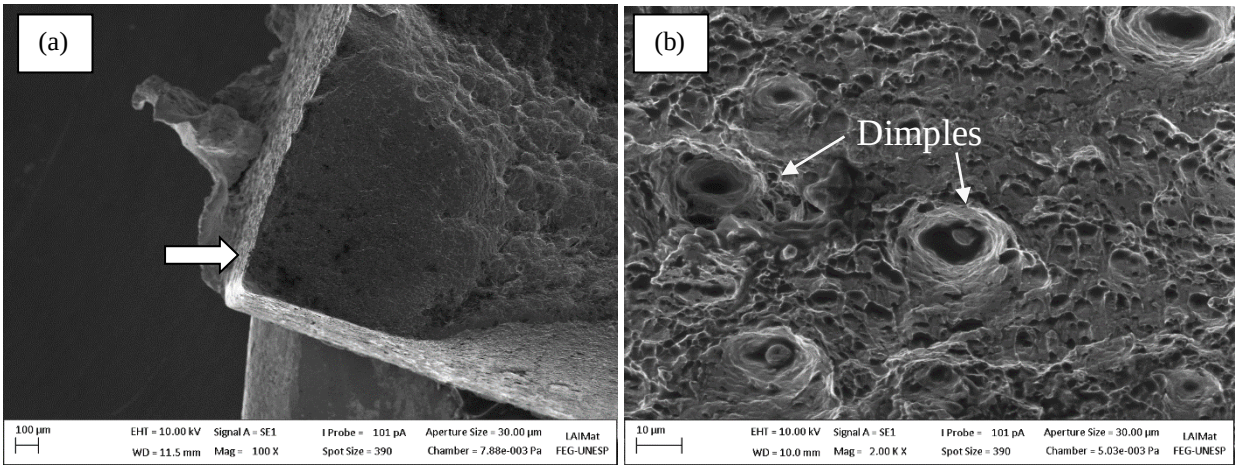

Figure 8. Fatigue fracture surface of LNE 500 steel depicting the (a) nucleation (magnification of 100x) and (b) final fracture regions (magnification of 2,000x).

The typical fatigue fracture surface of PA6/GF60 composite specimens is displayed in Fig. 9. From Fig. 9a, it can be seen the high fraction of glass fibers applied in the composite, which correspond to 60% by weight of the material. The glass fibers are completely surrounded by the matrix and the "pull-out" phenomenon, when voids are observed instead of the fiber in some regions, was not observed. Thus, the fiber/matrix interface did not have a detrimental influence in the fatigue behavior. However, there are some regions where there is not a uniform distribution of fibers (Fig. 9b), which may have affected the fatigue behavior of the material.

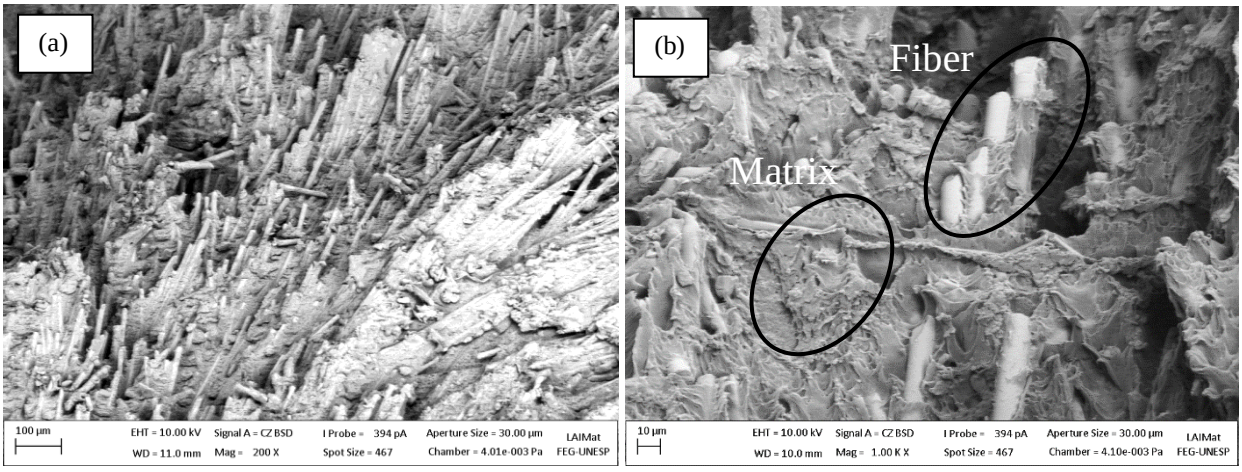

Figure 9. Fatigue fracture surface of PA6/GF60 composite. (a) Magnification of 200x and (b) magnification of 1,000x.

3.8 Finite element method (FEM)

Figure 10 shows the automotive stringer finite element analysis with the substitution of LNE 500 steel for PA6/GF60 composite for loading pairs of 500 N and 1,000 N forces applied in opposite directions. Comparing Fig. 10a and Fig. 10b, the maximum stress of the composite structure, 53.1 MPa, was inferior to the stress supported by the steel structure, 143.3 MPa. It is desirable for an optimum design that the steel structure withstand the maximum stresses since it has a higher mechanical strength than the PA6/GF60 composite. In the case of a loading pair of 1,000 N, the maximum stress in the composite structure was 88.4 MPa (Fig. 10c). It is important to notice that the maximum stresses

in the composite structure were located at regions of stress concentrations, especially in the connection of the steel and composite structures. Thus, optimization of design and changes in the connection type of structures could significantly reduce the effect of stress concentration, and, consequently, increase the reliability and service life of the component.

Considering that a cyclic loading with the maximum stress of 53.1 MPa was applied to the composite structure, the fatigue life estimated by Eq. (4) would be about 3.4 x 10^4 cycles. However, for a maximum stress of 88.4 MPa, the predicted fatigue life would be only 2.4 x 10^3 cycles. Therefore, the PA6/GF60 composite is not recommended for structural automotive parts that are subjected to variable or cyclic loadings of a high maximum stress level. However, it could still be applied in the design of a component partially made of PA6/GF60 composite in order to reduce the weight of the component with the necessary design modifications to withstand the loadings.

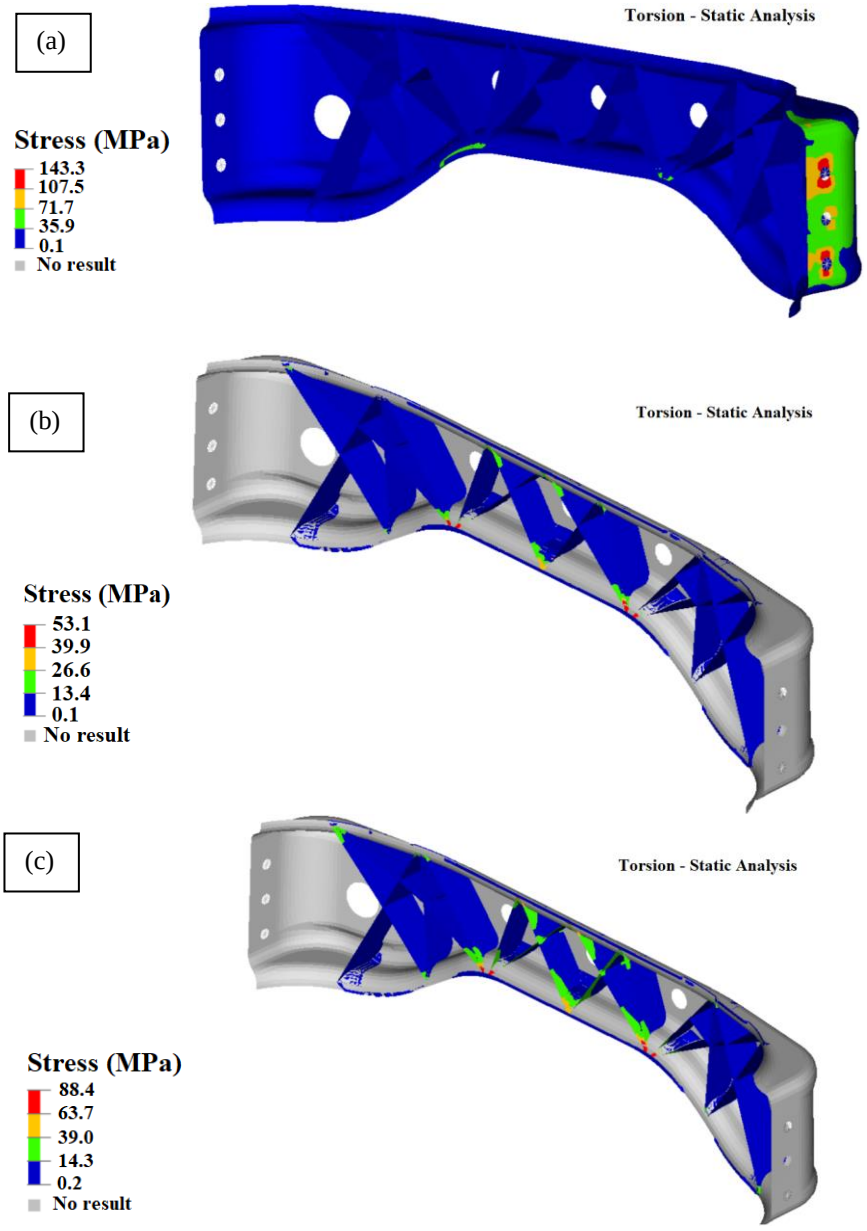

Figure 10. Automotive stringer finite element analysis for (a) a pair of 500 N forces, (b) a pair of 500 N forces (composite structure only), and (c) a pair of 1,000 N forces, showing results only in the composite structure.

4. CONCLUSION

The mechanical, fatigue and thermal properties of 60% glass fiber reinforced polyamide 6 were investigated and comparted to mechanical and fatigue properties of LNE 500 steel. The feasability of the substituion of LNE 500 steel for PA6/G60 composite was evaluated.

The tensile properties of LNE 500 were superior to PA6/G60. However, the mass index values indicate the weight and lifetime energy consumption reduction potential of applying PA6/G60 composite for automotive components as a substitution for original projects made with steel. The influence of fiber orientation on the mechanical properties was noted since the composite had better flexural strength in the parallel direction to the fiber orientation than perpendicular direction. The T_g temperature of the material was relatively low and it may be a critical factor considering that the automotive stringer may reach higher temperatures. Besides, the substitution of steel for the composite studied would result in a significant reduction of the fatigue strength of the component. The PA6/GF60 composite is not recommended for structural automotive parts that will have to withstand dynamic loadings of a high maximum stress level. The substitution of steel for lightweight composite materials for automotive structural applications may lead to the necessity of new design concepts.

5. ACKNOWLEDGEMENTS

This study was financed in part by the Coordenação de Aperfeiçoamento de Pessoal de Nível Superior - Brasil (CAPES) - Finance Code 001. The authors acknowledge Maxion SC for the material provided.

6. REFERENCES

Bernasconi, A., Davoli, P., Basile, A. and Filippi, A.V., 2015. “Effect of fibre orientation on the fatigue behaviour of a short glass fibre reinforced polyamide-6”. *International Journal of Fatigue*, Vol. 29, pp. 199–208.

Gendre, L., Njuguna, J., Abhyankar, H. and Ermini, V., 2015. “Mechanical and impact performance of three-phase polyamide 6 nanocomposites”. *Materials and Design*, Vol. 66, pp. 486–491.

Güler, T., Demirci, E., Yildiz, A. R. and Yavuz, U., 2018. “Lightweight design of an automobile hinge component using glass fiber polyamide composites”. *Materials Testing*, Vol. 60, N. 3, pp. 306–310

Güllü, A., Özdemir, A. and Özdemir, E., 2006. “Experimental investigation of the effect of glass fibres on the mechanical properties of polypropylene (PP) and polyamide 6 (PA6) plastics”. *Materials & Design*, Vol. 27, N. 4, pp. 316–323.

Kampe, S.L., 2001. “Incorporating Green Engineering in Materials Selection and Design”. In *Proceedings of The 2001 Green Engineering Conference: Sustainable and Environmentally-Conscious Engineering*. Roanoke, United States.

Koplin, J., Seuring, S. and Mesterharm, M., 2007. “Incorporating sustainability into supply management in the automotive industry - the case of the Volkswagen AG”. *Journal of Cleaner Production*, Vol. 15, pp. 1053–1062.

Mayyas, A., Qattawi, A., Omar, M. and Shan, D. “Design for sustainability in automotive industry: A comprehensive review”. *Renewable and Sustainable Energy Reviews*, Vol. 16, pp. 1845–1862.

Mouti, Z., Westwood, K., Long, D. and Njuguna, J., 2013. “An experimental investigation into localised low-velocity impact loading on glass fibre-reinforced polyamide automotive product”. *Composite Structures*, Vol. 104, pp. 43–53.

O’Brien-Bernini, F., 2011. “Composites and sustainability — when green becomes golden”. *Reinforced Plastics*, Vol. 55, N. 6, pp. 27–29.

Ishikawa, T., Amaoka, K., Masubuchi, Y., Yamamoto, T., Yamanaka, A., Arai, M. and Takahashi, J., 2018 “Overview of automotive structural composites technology developments in Japan”. *Composites Science and Technology*, Vol. 155, pp. 221–246.

Teixeira, D., Giovanela, M., Gonella, L.B. and Crespo, J.S,, 2015. “Influence of injection molding on the flexural strength and surface quality of long glass fiber-reinforced polyamide 6.6 composites”. *Materials and Design*, Vol. 85, pp. 695–06.

Tisza, M., Czinege, I., 2018. “Comparative study of the application of steels and aluminium in lightweight production of automotive parts”. *International Journal of Lightweight Materials and Manufacture*, Vol. 1, pp. 229–238.

Sasayama, T., Okabe, T., Aoyagi, Y. and Nishikawa, M., 2013. “Prediction of failure properties of injection-molded short glass fiber-reinforced polyamide 6,6”. *Composites: Part A*, Vol. 52, pp. 45–54.

7. RESPONSIBILITY NOTICE

The authors are the only responsible for the printed material included in this paper.